High Energy Density Physics 7 (2011) 150–154

Contents lists available at ScienceDirect

High Energy Density Physics

journal homepage: www.elsevier.com/locate/hedp

Gamma ray spectra from targets irradiated by picosecond lasers

J.F. Seely [a,*], C.I. Szabo [b], Uri Feldman [b], Hui Chen [c], L.T. Hudson [d], A. Henins [d]

[a] Naval Research Laboratory, Washington, DC 20375, USA
[b] Artep Inc., 2922 Excelsior Spring Circle, Ellicott City, MD 21042, USA
[c] Lawrence Livermore National Laboratory, Livermore, CA 94550, USA
[d] National Institute of Standards and Technology, Gaithersburg, MD 20899, USA

ARTICLE INFO

Article history:
Received 8 April 2011
Accepted 8 April 2011
Available online 15 April 2011

Keywords:
Gamma ray
Positron
Picosecond laser

ABSTRACT

Photon spectra in the energy range 60 keV to 1 MeV were recorded from targets irradiated by the LLNL Titan and LLE EP picosecond lasers. The radiation consisted of K-shell radiation, bremsstrahlung radiation from MeV electrons, and preliminary evidence for 511 keV positron annihilation radiation. The spectra were recorded by two instruments, an energy-dispersive CCD detector with a CsI phosphor coating that operated in the single-hit per pixel mode and was absolutely calibrated using a Cs-137 662 keV source, and a wavelength-dispersive Cauchois type spectrometer employing a curved Ge(220) transmission crystal that operated in the first and second diffraction orders with high spectral resolution. The calibrated photon energy distributions from Au, Eu, and Al targets are compared to the energetic electron distributions emerging from the targets.

Published by Elsevier B.V.

1. Introduction

When focused to a few micron diameter, a powerful laser pulse (>100 TW) has electric field strength >30 MV/μm and can accelerate electrons in solid material on fsec time scales to MeV energies. In high-Z materials such as gold, these electrons slow down within a mm and produce intense hard X-ray bremsstrahlung radiation. This in turn can create electron-positron pairs when target nuclei interact directly with such energetic electrons (the trident process) [1] or indirectly with energetic bremsstrahlung photons (the Bethe–Heitler process) [2]. High-energy electrons and positrons have been observed to emerge from gold and other targets, where acceleration results from the intense sheath field particularly at the backside of relatively thin targets, and beams of energetic electrons and positrons were produced by shaping the backside surface [3].

While the study of energetic particles emerging from solid density targets can provide useful information about the laser-target interaction, the inferred particle parameters are not necessarily characteristic of the energy distributions inside the target owing to the slowing down process and to acceleration at the surface. A better indication of the energy distribution inside the target is gained by the study of the energetic radiation emerging from the target such as MeV X-rays and 511 keV positron annihilation radiation. As indicated in Fig. 1, the radiation with energy >300 keV undergoes low attenuation while escaping from mm size gold targets. By use of transmission crystal spectrometers and targets having several heavy metal wires distributed within the targets, the hard X-ray K-shell spectra were recorded and were utilized to infer the energies of electrons generated in the focal spot and propagation over mm distances from the focal spot in a variety of materials [4,5].

In this paper, we report the observation of MeV gamma ray spectra from gold and other targets irradiated by the LLNL Titan and the LLE EP picosecond lasers. The gamma ray fluence is compared to the energetic electron and positron fluences emerging from the targets. These results, when combined with numerical modeling, can be used to characterize the positron creation and annihilation mechanisms inside the target.

2. Single-hit CCD detector

The gamma ray spectra were recorded by a CCD detector having 1700 by 1200 pixel format, 20 μm pixel size, and a CsI scintillator [6]. The detector was calibrated using the K-shell lines from a W discharge source [7], and more recently calibrations were performed using a Cs-137 radioactive source having 1.0×10^{11} Bq activity at 662 keV. When exposed to the Cs-137 source, it was found that numerous individual pixels had high counts and were surrounded by pixels with low background counts. The number of bright pixels was proportional to the integration time, decreased with source to detector distance as R^{-2}, and decreased with added lead or tungsten shielding as expected for attenuation of 662 keV

* Corresponding author. Tel.: +1 202 767 3529.
E-mail address: john.seely@nrl.navy.mil (J.F. Seely).

1574-1818/$ – see front matter Published by Elsevier B.V.
doi:10.1016/j.hedp.2011.04.002

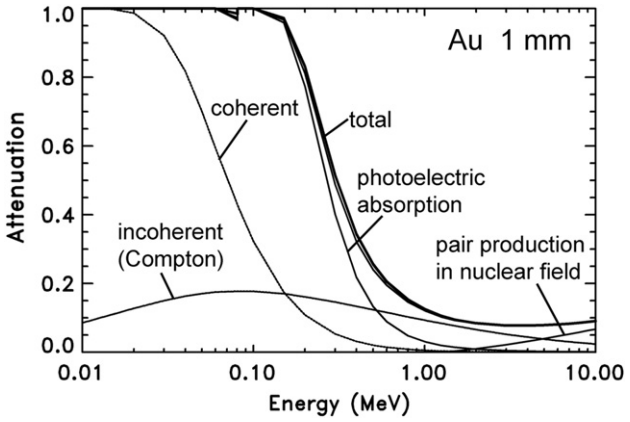

Fig. 1. Photon attenuation in 1 mm thick Au calculated by the NIST XCOM code.

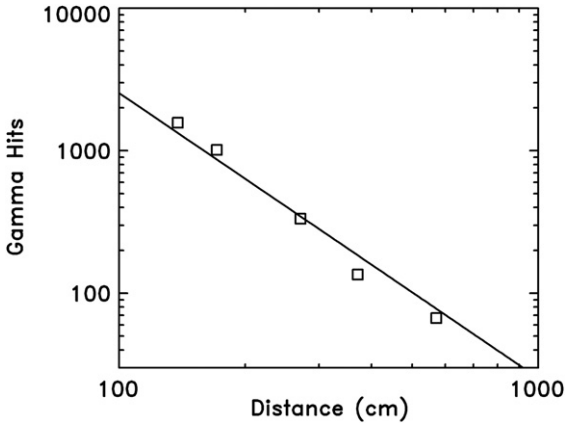

Fig. 2. The data points are gamma hits recorded by the CCD detector using the 662 keV Cs-137 radioactive source and 10 s integration time as functions of the source to detector distance. The curve was calculated using the photoelectric absorption of 662 keV gammas in the CCD's CsI scintillator.

photons. The individual bright pixels are therefore interpreted as resulting from single 662 keV photons.

The number of 662 keV gamma hits in a 500×500 pixel region during 10 s exposures for source to detector distances in the 138 cm to 571 cm range is shown by the data points in Fig. 2. At the smallest distance, only 0.6% of the pixels have gamma hits, and thus the probability of multiple gammas producing a hit is negligible. The curve in Fig. 2 was calculated using the 0.031% photoelectric absorption in 60 μm thick CsI. The average deviation of the data points from the curve is 12%, and this represents the uncertainty in the measurements.

The histogram of the number of pixels versus the counts per hit was calibrated using the conversion factor 125 counts/662 keV photon which was consistent with the conversion factor for 60 keV W K lines [7]. This conversion factor was used to convert the histogram of hits to an energy spectrum in the Titan and EP laser experiments.

3. Spectra from Titan shots

The CCD detector was positioned outside the Titan laser-target chamber at a distance of 2.85 m from the target. The detector had a clear line of sight to the target through a Lexan vacuum window. The detector was housed in a lead shielded box with a viewing aperture and a lead tube collimator facing toward the Titan chamber window and the target. The viewing aperture was covered by a thin aluminum plate to make the box a Faraday enclosure, and CCD images were acquired on each Titan shot without electromagnetic interference (EMI). When the CCD box and collimator were positioned just outside the Titan chamber window, at a distance of 1.22 m from the target, EMI occurred on some shots and those data are not discussed here except to say that the number of gamma hits varied with distance from the target as R^{-2} for the two distances 1.22 m and 2.85 m.

Disk-shaped targets 1 mm thick and 2 mm in diameter were irradiated by a laser pulse having 10 ps duration and energy in the 200–350 J range. On some shots the target was also irradiated by an additional laser pulse having 3 ns duration and <10 J energy to create a longer scale-length plasma to investigate the effect on the generation of positrons and gammas, and for the data presented here the two pulses were focused to the same spot and arrived simultaneously.

Shown in Fig. 3 is a 400×600 pixel region of the CCD image recorded on Titan shot 31 having 349 J short-pulse energy and 9.6 J long-pulse energy on an Au target. Indicated are the (open) region of the image having no added attenuation filters, a region with 0.9 mm lead, and a region with 12.7 mm lead. The open region has 0.051 average gamma hits per pixel, and the hits in the filtered regions are smaller. These images had an additional step wedge of 0.9 mm lead with x1, x2, and x4 thicknesses, and it was verified that the hits/pixel decreased with increasing lead thickness characteristic of >100 keV photons from the target and passing through the Lexan vacuum window.

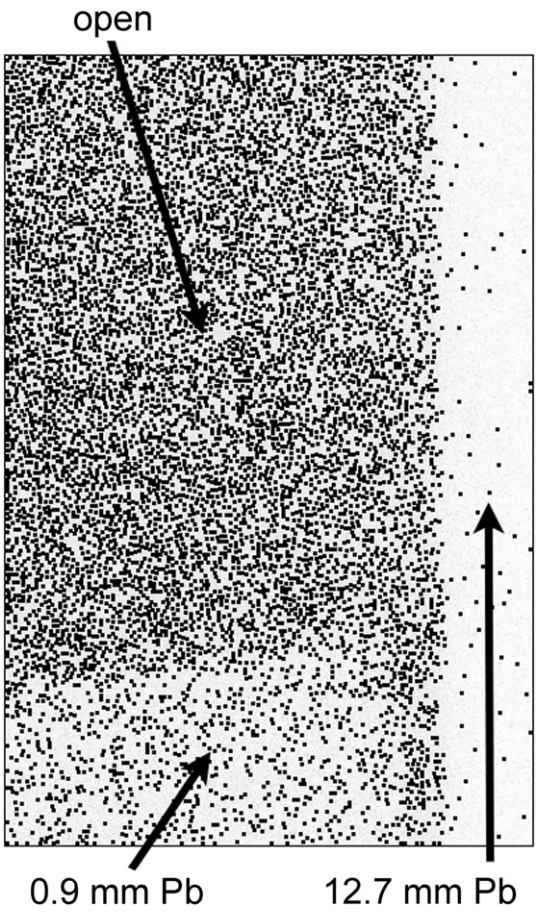

Fig. 3. Gamma ray hits produced by the Titan shot 31 having 349 J short-pulse energy and 9.6 J long-pulse energy in the open CCD region and regions having 0.9 mm Pb and 12.7 Pb added attenuation filters.

Shown in Fig. 4(a) are the total numbers of photons emitted from the targets, irradiated by varying short-pulse energies, as determined from the pixel hits in the open regions of the CCD images (without added attenuation filters). The data are corrected for transmission through the Lexan vacuum window and the air path to the detector and assume isotropic emission. The data points are identified by the Titan shot numbers in the range 31–38, the target material (Au, Eu, or Al), and, when present, the long-pulse energy. It is apparent from Fig. 4(a) that the number of emitted photons increases with the short-pulse energy and with the long-pulse energy. In addition, the number of emitted photons increases with the atomic number of the target, approximately proportional to Z.

Shown in Fig. 5 are the energy spectra determined from the calibration of the CCD detector using the Cs-137 source at 662 keV. The energy scale was established by the conversion factor of counts per energy absorbed by the photoelectric process in the CsI scintillator from the Cs-137 calibration and assuming a linear relationship between the counts and absorption at other energies. This is an approximate energy scale that should be improved by calibrations at energies in addition to 662 keV; however, the energy scale is sufficiently accurate to make comparisons among the spectra from the Titan and EP shots. The spectra are in units of photons/keV/sr emitted by the target, corrected for transmission through the Lexan vacuum window and the air path to the detector and assuming isotropic emission.

Fig. 5(a) shows the spectra from Titan shot 31, a Au target irradiated by 349 J short-pulse energy and 9.6 J long-pulse energy and from three regions: open (no added attenuation filters), 3.6 mm lead, and 12.7 mm lead. Straight lines are drawn through the data points in the high-energy tail of the spectra to indicate differences in slope. It is seen that with the added attenuation, the numbers of detected photons decrease and the tails of the spectra have decreasing slopes. Spectra from Eu and Al targets, having similar trends with added attenuation, are shown in Fig. 5(b) and (c). In general, with increasing atomic number of the target, the number of photons increases, the spectra have higher energies, and the high-energy tail has smaller slope. This implies a hardening of the spectra and a more efficient gamma production mechanism in the focal spot with increasing atomic number.

The characteristic energies of the exponential falloff of the high-energy tails of the spectra are shown in Fig. 4(b), where the data points are identified in Fig. 4(a). Also shown in Fig. 4(b) are the weighted average energies in the spectra, where the weighting is by the photons/keV/sr values. This illustrates the hardening of the spectra with increasing short-pulse energy and increasing atomic number of the target, while the presence of the long-pulse has a smaller effect on the spectral hardness.

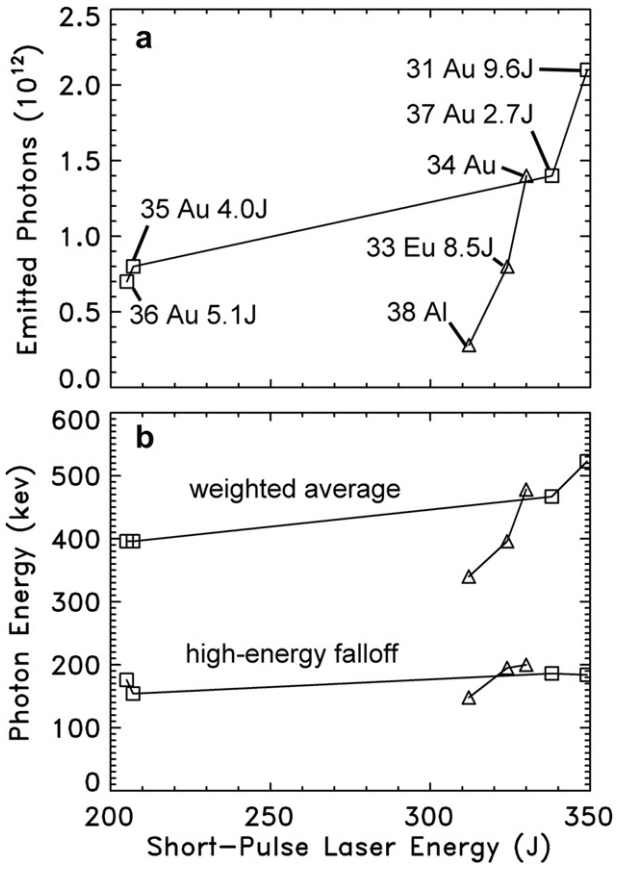

Fig. 4. (a) Photons emitted from the Titan shots (numbers 31–38) as functions of the short-pulse energy, long-pulse energy, and target atomic number. (b) Average weighted energies and the characteristic energies of the high-energy tails of the photon distributions.

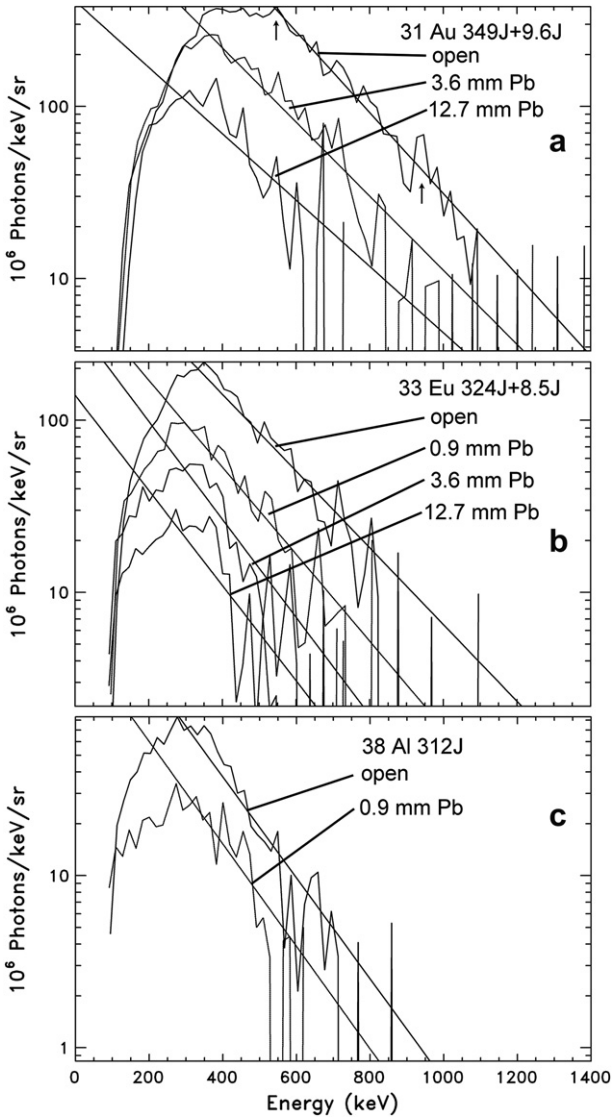

Fig. 5. Photon spectra from the Titan targets (a) Au, (b) Eu, and (c) Al. Straight lines are drawn through the data points in the high-energy tails of the photon spectra.

Shown in Fig. 6 are comparisons of (a) the gamma spectra from Au, Eu, and Al targets and (b) the energy distributions of the electrons emerging from the same targets. The electron spectra, and the positron spectra discussed later, were recorded by electron–positron–proton spectrometers (EPPS) as described in Ref. [8]. They were placed approximately 20 cm from the target to measure the energy spectra of the electrons and positrons emerging from the target. It is seen in Fig. 6 that both the photon and electron energies and numbers increase with the atomic number of the target. The electrons extend to higher energies because of acceleration by the electric sheath field at the target surface. The photon spectra are characteristic of the energy distributions inside the targets because of minimal attenuation in the targets.

4. Spectra from EP shots

The CCD detector was placed outside the EP target chamber and had a clear line of sight to the target through the 6.7 cm thick aluminum chamber wall. The CCD acquired images when placed 3.7 m from the chamber wall and suffered EMI when placed closer to the chamber wall.

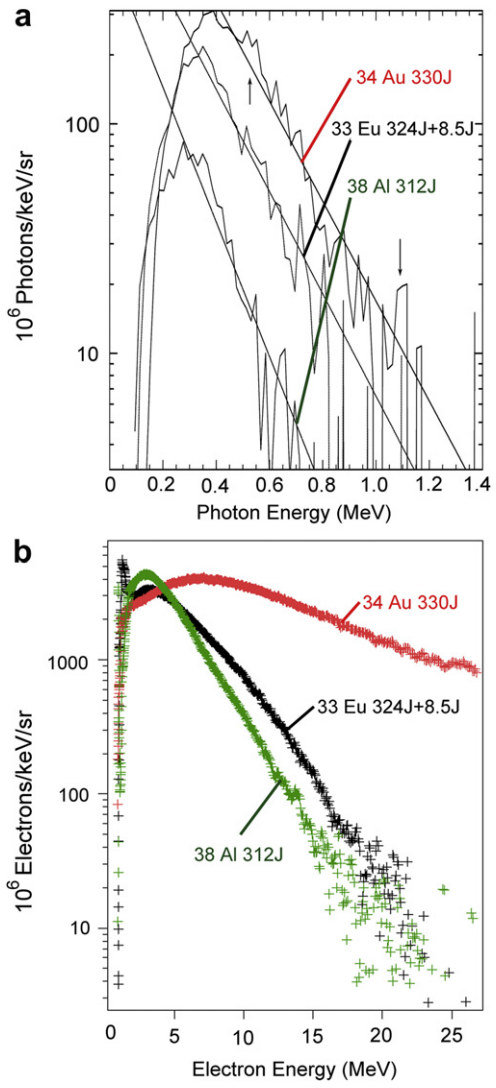

Fig. 6. (a) Photon spectra from Titan irradiated Au, Eu, and Al targets. (b) Distributions of energetic electrons escaping from the targets on the same Titan shots.

Gold disk targets 1 mm thick and 2 mm in diameter were irradiated by the EP side-lighter and back-lighter beams having 9.5 ps durations, overlapping focal spots, and simultaneous arrival. Shown in Fig. 7(a) is the gamma ray spectrum from a shot having 759 J side-lighter energy and 843 J back-lighter energy compared to the spectrum from the Titan shot 31 having 349 J short-pulse energy and 9.6 J long-pulse energy. The EP spectrum is corrected for the transmission through the EP chamber wall and air path to the detector and assumes an isotropic distribution. Shown in Fig. 7(b) are the energetic electrons and positrons emerging from the EP target.

The Titan shot produced 2.1×10^{12} gammas and the EP shot produced 3.2×10^{13} gammas, a factor of 15 more gammas produced by a factor of 4.5 higher energy. This implies that the number of gammas increases non-linearly with laser energy and intensity, also indicated by the Titan data at higher energies as shown in Fig. 4(a).

5. Positron annihilation radiation

A goal of this research is to spectrally resolve the positron annihilation photons near 511 keV. The accurate measurement of the energy and width of the 511 keV spectral feature would be a measure of the slowing down of the positrons inside the target and would inform the positron production and annihilation mechanisms. While there are small bumps in the CCD spectra near 511 keV and at twice that energy in the spectra from the Au targets, as indicated by the arrows in Figs. 5(a) and 6(a), the spectral features are near the noise level and are inconclusive. The inherent low energy resolution of the single-hit CCD spectra also inhibits the observation of the 511 keV feature.

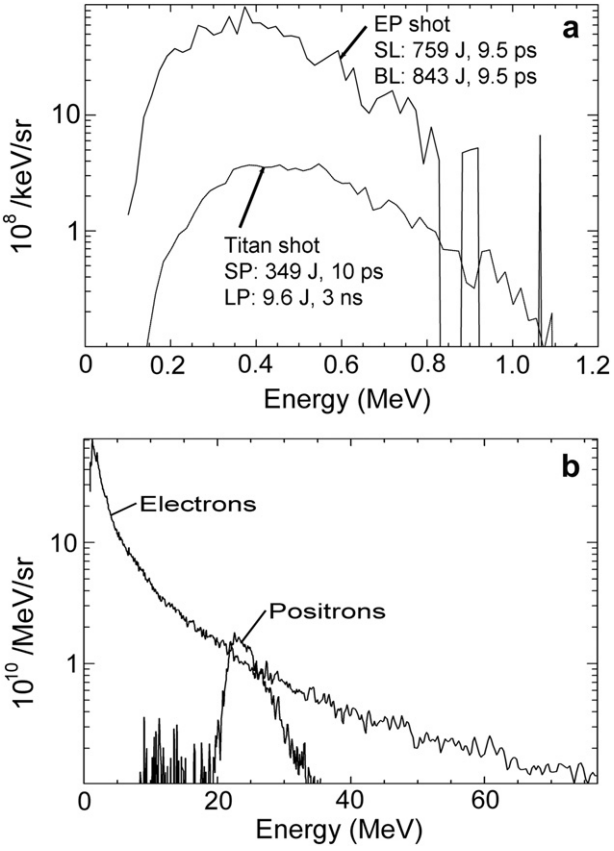

Fig. 7. (a) Comparison of the photon spectra from an EP shot and a Titan shot. (b) Energetic electrons and positrons escaping from the EP target.

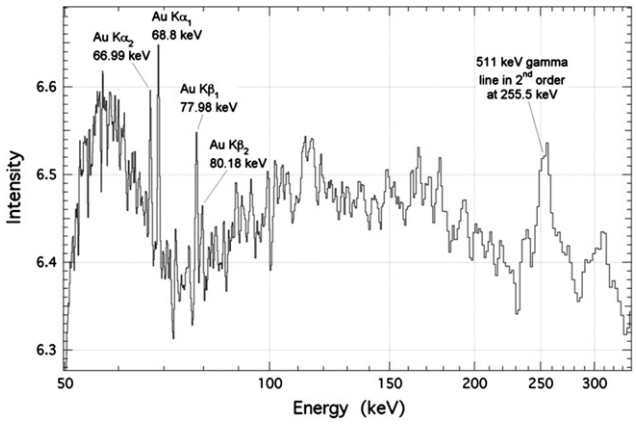

Fig. 8. High-resolution spectrum recorded by a transmission crystal spectrometer from an Au target irradiated by the Titan laser.

A high-resolution transmission crystal spectrometer was designed and fielded on the Titan laser shots discussed in Section 3. The spectrometer achieved the high dispersion necessary to observe 511 keV photons by using a Ge (220) crystal having a relatively small lattice spacing (0.200 nm) and bent to a large Rowland circle diameter (965 mm). Compared to previous transmission crystal spectrometers successfully utilized at laser facilities [5], the instrument sensitivity was increased by employing a small source to crystal standoff distance (254 mm) and a relatively thick Ge crystal (0.4 mm). The spectra were recorded on Fuji MS image plates, and the sensitivity of the image plate and scanner was calibrated at 662 keV using the Cs-137 source. The spectrometer bandwidth includes the Au K-shell lines in the 67–80 keV range in the first diffraction order and the 511 keV region in the second order. The energy scale was accurately determined, and the shielding against scattered photons was optimized, using the K-shell lines and high-energy continuum from a W laboratory source with 400 kV peak kilovoltage.

Spectral features at 511 keV were observed on many Titan laser shots on Au disk targets (1 mm thick, 2 mm diameter) but were not observed on all Au shots. An example spectrum is shown in Fig. 8 where the first-order Au K lines and the second-order 511 keV feature are identified. The high-energy scattered photon level was high in all spectra, comparable to the scattered photon level in spectra recorded from the NRL Gamble 2 MeV discharge machine with a similar spectrometer [7]. The identification of the 511 keV spectral feature must be confirmed by additional laser shots and by further improvements in the spectrometer sensitivity and suppression of the background level. The spectrometer sensitivity can be increased by use of a thicker crystal having higher atomic number (higher coherent scattering cross-section), and these improvements are underway.

6. Discussion

We have presented the first calibrated gamma ray spectra, up to approximately 1 MeV, produced by the irradiation of millimeter size gold targets by intense picosecond laser pulses. The numbers and energies of the gamma rays are correlated with the laser energy and with the atomic number of the target as well as with the numbers of energetic electrons escaping from the target. Evidence is presented for the observation of the 511 keV positron annihilation feature in the spectra recorded by a high-resolution transmission crystal spectrometer.

In contrast to the escaping electrons and positrons, which slow down inside the target and are accelerated by the sheath field at the target surface, the gamma ray spectra experience low attenuation while escaping the target and are characteristic of the energy distribution inside the target. Continued improvement in the sensitivity and spectral resolution of the instrumentation, as well as the increased X-ray continuum and 511 keV fluences produced by short-pulse lasers with increasing energy and focused intensity, will enable the accurate measurement of the energy and width of the 511 keV spectral feature and characterization of the positron creation and annihilation mechanisms inside the high-Z solid density targets.

Acknowledgements

We thank Drs. J. Schumer, C. Boyer, and N. Pereira of the NRL Plasma Physics Division for contributions to the CCD detector. The work at NRL was supported by the Office of Naval Research. H. C. was funded under the auspices of the U.S. DOE by LLNL under DE-AC52-07NA27344. Certain commercial equipment, instruments, or materials are identified in this paper in order to specify the experimental procedure adequately. Such identification is not intended to imply recommendation or endorsement by the U.S. government, nor is it intended to imply that the materials or equipment identified are necessarily the best available for the purpose.

References

[1] J.W. Shearer, J. Garrison, J. Wong, J.E. Swain, Phys. Rev. A 8 (1973) 1582.
[2] H. Chen, et al., Phys. Rev. Lett. 102 (2009) 105001.
[3] H. Chen, et al., Phys. Rev. Lett. 105 (2010) 015003.
[4] J. Seely, et al., High Energy Density Phys. 5 (2009) 263.
[5] J. Seely, et al., Phys. Plasmas 17 (023102) (2010).
[6] J. Seely, et al., Appl. Opt. 49 (2010) 4372.
[7] N. Pereira, et al., Rev. Sci. Instr. 81 (2010) 10E302.
[8] H. Chen, et al., Rev. Sci. Instr. 79 (2008) 10E533.